LWT - Food Science and Technology 166 (2022) 113765

Contents lists available at ScienceDirect

LWT

journal homepage: www.elsevier.com/locate/lwt

Techno functional characterization of green-extracted soluble fibre from orange by-product

Claudia Perez-Pirotto [a,b,*], Gemma Moraga [b], Amparo Quiles [b], Isabel Hernando [b], Sonia Cozzano [a], Patricia Arcia [a,c]

[a] Departamento de Ingeniería, Universidad Católica del Uruguay. Montevideo, 11600, Uruguay
[b] Food Microstructure and Chemistry Research Group, Department of Food Technology, Universitat Politècnica de València, Valencia, 46022, Spain
[c] Latitud Latu Foundation. Montevideo, 11500, Uruguay

ARTICLE INFO

Keywords:
Orange pomace
Techno functional properties
Soluble dietary fibre
Microstructure

ABSTRACT

This work studies the techno-functional properties of the spray dried water-soluble extracts from orange pomace, obtained from different green extraction technologies. Orange pomace, a by-product from the juice production industry, was used for soluble fibre extraction. Starting from pomace, four extraction procedures were assayed: hot water, extrusion + hot water, jet cooker and jet cooker + hot water. After treatments, the supernatant was spray dried with whey protein isolate to obtain soluble fibre enriched powders. Microstructure by field emission scanning electron microscopy, color, particle size, moisture content, hydration properties, foaming capacity and stability, rheology, and glass transition temperatures were assayed. All powders exhibited an orange shade. In microstructure, particle size, and glass transition temperature, the powder obtained from extrusion + hot water presented a different behavior from the other powders: less caking and agglomeration, and smaller particles. Also, this powder showed the highest foaming stability and viscosity, as well as glass transition temperature, properties that make it interesting for the food industry. Through valorization of orange pomace fiber-enriched powders could be obtained; these powders can be used as ingredients in the industry to address the fibre gap and provide technological functionalities.

1. Introduction

Dietary fibre is a class of compounds that includes a mixture of plant carbohydrate polymers resistant to digestion by human small intestinal enzymes (O'Keefe, 2019). The intake of these compounds has numerous documented health benefits, such as reduced risk of coronary heart disease, diabetes and obesity, among others. Also, fibre, especially the soluble type, is well reputed for its ability to lower blood lipid levels (Elleuch et al., 2011).

However, there is a worldwide shortage on its consumption, despite its health effects being well known. Although there is no consensus on recommended daily intake, both EFSA and FAO recommend a minimum intake of 25 g/day. Notwithstanding consumers' efforts to increase it, they are not reaching it (Santos et al., 2022). For example, the USA currently has an intake of 16 g/day, while the UK has an intake of about 18 g/day (O'Keefe, 2019).

Dietary fibre is also appealing from the technological point of view, as it exhibits some properties that make it an interesting ingredient to add to products. Examples of these are water and oil holding capacity, increasing viscosity and emulsification, among others (Dhingra et al., 2012; Elleuch et al., 2011). Fibre has been added to various types of products, such as bread and sweet bakery products, as a substitute of wheat flour (Quiles et al., 2018). Studies have also been done with ice cream, where fibre played a cryoprotective role (Soukoulis et al., 2009). Fiber-enriched jams and meats have also been prepared, to avoid synaeresis and modify textural properties (Elleuch et al., 2011; Figueroa & Genovese, 2019).

Thus, dietary fibre is an ingredient that may be added to foods, not only to improve its nutritional value, but also because of its technological properties. Furthermore, supplementing massively consumed foods with dietary fibre is a good approach to address the fibre gap. This would result both in an increase of the daily intake, as well as a decrease of the intake of other ingredients, such as fats and synthetic emulsifiers, due to fibre aforementioned technological properties. Also, as consumers

* Corresponding author. Food Microstructure and Chemistry Research Group, Department of Food Technology, Universitat Politècnica de València, Valencia, 46022, Spain.
E-mail address: clpepi@upv.edu.es (C. Perez-Pirotto).

https://doi.org/10.1016/j.lwt.2022.113765
Received 26 April 2022; Received in revised form 3 June 2022; Accepted 9 July 2022
Available online 13 July 2022

prefer natural supplements, adding fibre is a good alternative to synthetic ingredients (Elleuch et al., 2011).

In this context, in recent years a trend to find new sources of fiber enriched ingredients has arisen (Majerska et al., 2019; Rodríguez et al., 2006). Fruit by-products, especially pomaces, are a good source of these ingredients. These could be used as a new product, or if processed, as a way of enriching food products with compounds that enhance their physical and chemical properties (Majerska et al., 2019). Citrus fruits are one of the top global agricultural commodities, with a global production in 2021/2022 estimated to be about 48.8 million tons of oranges (USDA Foreign Agricultural Service 2022). About 19 million tons of these are expected to be destined for processing, and around 50% w/w (wet weight) are seeds, peels and internal tissue (Wilkins et al., 2007), which means in 2021/2022 nearly 9.5 million tons of by-product will be produced. This waste has been reported as high in dietary fibre content and rich in several bioactive compounds, such as polyphenols and flavonoids (Gutiérrez Barrutia et al., 2019).

Several processes have been used for fibre extraction as a way of giving added value to by-products. These include not only chemical processes, but also enzymatic or physical processes. Current trends tend to look for extraction technologies without the use of solvents, the so-called "green technologies" (Chemat et al., 2012). Examples of these are enzyme assisted extractions in *Laminaria japonica* (Gao et al., 2017) and in flaxseed gum (Moczkowska et al., 2019), and steam explosion in sweet potato (Wang et al., 2017), in apple pomace (Liang et al., 2018), and in okara (Li et al., 2019). Ultrasound has also been used for fibre extraction flaxseed gum (Moczkowska et al., 2019) and combined with acid extraction for fibre extraction in papaya peel (Zhang et al., 2017). High hydrostatic pressures have been used for fibre modification in purple-fleshed potatoes (Xie et al., 2017). Extrusion has been extensively studied to improve the ratio IDF:SDF, for example in lupin seed coat (Zhong et al., 2019), in garlic skins (Guo et al., 2018) and in orange pomace (Huang & Ma, 2016).

The aim of this work was to evaluate the technological properties of soluble fiber enriched powder obtained from orange pomace applying different green extraction technologies, to be used as an ingredient in food fibre fortification.

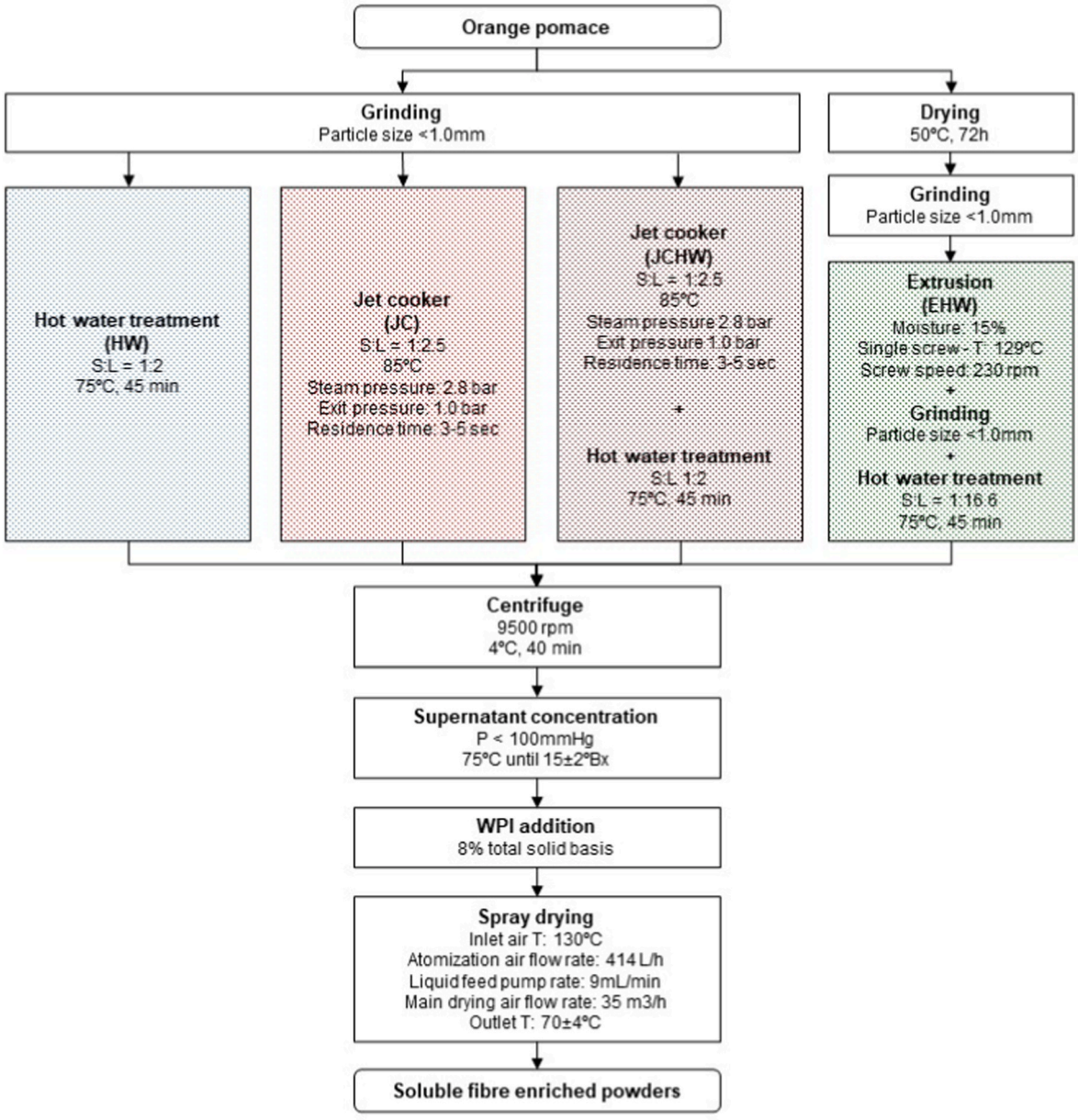

Fig. 1. Orange pomace's processing for fibre extraction.

2. Materials and methods

2.1. Soluble fibre enriched powders

Powders were obtained according to Perez-Pirotto et al., 2022, as presented on Fig. 1. Briefly, starting from orange pomace four different treatments were assayed in pilot scale equipment (hot water – HW, extrusion + hot water - EHW, jet cooker - JC, jet cooker + hot water - JCHW) to extract soluble fibre. After performing the different treatments, mixtures were centrifuged, supernatant was concentrated under vacuum and spray dried on a Buchi B290 spray dryer. Encapsulation was necessary to overcome stickiness in drying chamber. For this purpose, whey protein isolate (WPI – Provon 292, Glanbia Nutritionals Inc.) was added (8% total solids basis) to the concentrate before drying and was kept under magnetic stirring at 60 °C until completely dissolved. After spray drying, powders were stored under vacuum at room temperature in the dark until use.

Chemical composition of powders was analysed on a previous study (Perez-Pirotto et al., 2022). Briefly, TDF content was 9.48 ± 0.45 g/100 g dwb for HW, 20.20 ± 3.69 g/100 g dwb for EHW, 10.25 ± 0.89 g/100 g dwb for JC and 13.03 ± 1.8 for JCHW. Total sugars content was 64.15 ± 0.2 g/100 g dwb in HW, 46.15 ± 0.05 g/100 g dwb in EHW, 64.24 ± 0.13 g/100 g dwb in JC and 60.37 ± 0.31 g/100 g dwb in JCHW.

2.2. Microstructure

Samples were observed by Field Emission Scanning Electron Microscopy (FESEM). The sample was adhered to double-sided carbon tape and sputtered with a thin platinum layer. Samples were then photographed (Ultra 55 FESEM, Zeiss, Oberkochen, Germany) with an accelerating voltage of 1.5 kV.

2.3. Color

Powder color was measured with a LabScan XE (HunterLab, USA). Results were expressed as Hunter color values, L*, a* and b*. L* denotes lightness and darkness, a* redness and greenness, and b* yellowness and blueness. Chroma (ΔC) and Hue angle (°) were also calculated, following equations (1) and (2). Browning index, which is indicative of the brown color, an important parameter where browning reactions may take place, was calculated as suggested by Phuon et al., 2021, with equation (3).

$$Chroma = (a^{*2} + b^{*2})^{\frac{1}{2}} \quad (1)$$

$$Hue\ angle\ (H) = tan^{-1}(\frac{b^*}{a^*}) \quad (2)$$

$$Browning\ Index = \frac{[100\frac{(a+1.75L)}{(5.645L+a-3.012b)} - 0.31]}{0.17} \quad (3)$$

2.4. Particle size

A particle size analyzer (NanoPlus zeta potential and particle size analyzer, Particulate Systems, Atlanta, GA) was used to determine particle size distribution. Samples were suspended in distilled water and particle size was determined by light scattering. Distribution is expressed in terms of differential volume at a certain diameter. Also, D_{10}, D_{50} and D_{90} were calculated, where D_x represents the diameter for which x% of the particles have a smaller size. Span was calculated according to Fournaise et al., 2021.

2.5. Water content and hydration properties

2.5.1. Water content

The water content of the samples was obtained by vacuum drying the samples in a vacuum oven at 60 °C and a pressure <100 mmHg, until constant weight.

2.5.2. Water solubility

Water solubility was assayed according to Wang et al. (2015). Briefly, 0.5 g were accurately weighed (W) in a Falcon tube and 25 mL of distilled water were added. Tubes were vortexed at high speed for 30 s and left at 90 °C for 30 min, with agitation, and afterwards centrifuged at 9000 rpm for 10 min. Supernatant was lyophilized and weighed (W_1). Water solubility was calculated according to the following formula:

$$WS\ (\%) = \frac{W_1}{W} \times 100 \quad (4)$$

2.5.3. Hygroscopicity

Hygroscopicity was evaluated following the method proposed by Oliveira et al. (2018). One (1.0) gram of sample was accurately weighed in glass Petri dishes, in duplicate (W_i), and placed in a hermetic container containing a glass with saturated NaCl solution, to get 75.5% humidity. This container was left at room temperature (20 °C) standing for one week. Petri dishes were afterwards weighed (W_f) and hygroscopicity was expressed as grams of adsorbed moisture per 100 g of sample, using equation (5):

$$Hygroscopicity = \frac{W_f - W_i}{W} \times 100 \quad (5)$$

2.5.4. Oil holding capacity (OHC)

Oil holding capacity was performed according to Wang et al. (2015), with modifications. 0.5 g were accurately weighed (W) in a previously weighed centrifuge tube. 5 mL of sunflower oil were added and mixed. Tubes were left standing at room temperature for 1 h. Samples were centrifuged at 4200 rpm for 15 min. Sediment was weighed (W_1) and OHC was calculated according to the following formula:

$$OHC\ (\frac{g}{g}) = \frac{W_1}{W} \quad (6)$$

2.6. Foaming capacity

Foaming capacity was assayed following Dick et al. (2019) method, with some modifications. One (1.0) gram of sample was weighed in a flask and 50 mL of distilled water were added. Samples were kept overnight at 4 °C to ensure complete hydration. Volume was measured before whipping (V_b) Afterwards, the sample was homogenized with ultraturrax for 2 min at 10000 rpm and quickly transferred to the same graduated tube in which volume was previously measured. Volume of the foam was recorded (V_a). Foaming capacity (FC) was calculated according to the following formula:

$$FC(\%) = \frac{V_a - V_b}{V_b} \times 100 \quad (7)$$

For foam stability, foam volume was measured 5, 10, 30 and 60 min after whipping, and foaming capacity was calculated.

2.7. Rheology

Rheological properties were tested on a Rotational Rheometer (Kinexus Pro+, Malvern Panalytical, Worcestshire, UK) equipped with a Peltier cartridge to control sample's temperature. Concentric cylinders were used.

Solutions at 8% (w/w) concentration were prepared the day before and left at 4 °C to ensure proper hydration of the samples. The day of the test, samples were removed from the refrigerator and left at room temperature to reach equilibrium.

Viscosity of the samples was analysed at 25 °C using shear rate from 0.1 to 200 s^{-1} during 180 s. Samples were allowed to reach equilibrium

for 3 min before starting analysis.

2.8. Differential scanning calorimetry

Glass transition temperature was determined using Differential Scanning Calorimetry (DSC25 - TA Instruments, New Castle, Delaware USA). Around 10 mg of powder were accurately weighed in aluminum pans (Tzero pans – TA Instruments, New Castle, Delaware, USA) and sealed. Samples were equilibrated at 20 °C, cooled to −20 °C, and then heated to 60 °C at 10 °C/min in an inert atmosphere. An empty pan was used as a reference, and liquid nitrogen was used for sample cooling. Glass transition temperature was evaluated at the midpoint of the transition, using TRIOS Software (TA Instruments, New Castle, Delaware, USA).

2.9. Statistical analysis

Analyses were performed in duplicate. Results are expressed as mean ± SD. ANOVA analyses were performed, and differences between samples were determined by LSD Fisher test with p-value 0.05.

XLSTAT 2021.2.1 software (Addinsoft 2020; New York, NY, USA). was used for data processing.

3. Results and discussion

3.1. Microstructure

After spray drying particles tend to be spherical, as this is the most stable droplet formation (Gagneten et al., 2019). Micrographs of the spray dried product are shown on Fig. 2. In this case, particles are rather spherical, although some shrinkage is observed. Temperatures below 140 °C render particles with wrinkled surfaces (Ferrari et al., 2012); so, taking into account drying operating conditions shrinkage may be due to drying inlet temperature.

In all cases, coalescence is observed: particles have agglomerated and formed greater irregular particles, as can be seen in Fig. 2. However, this is more evident in the case of JC and JCHW (Fig. 2E–H), and to a lower degree in HW and EHW powder (Fig. 2A–D). In the latter case, the fusion of two or more particles is not as notorious as in the first cases: particles keep their individual shape and have not coalesced. The fusion of particles is due to the liquid bridges established that connect particles with each other, which are formed using available moisture or absorbing the moisture from the environment (Edrisi Sormoli & Langrish, 2016). As this is part of the caking that is produced in sugars, EHW is expected to be the powder with the least fusion, as it is the one with the lowest sugar

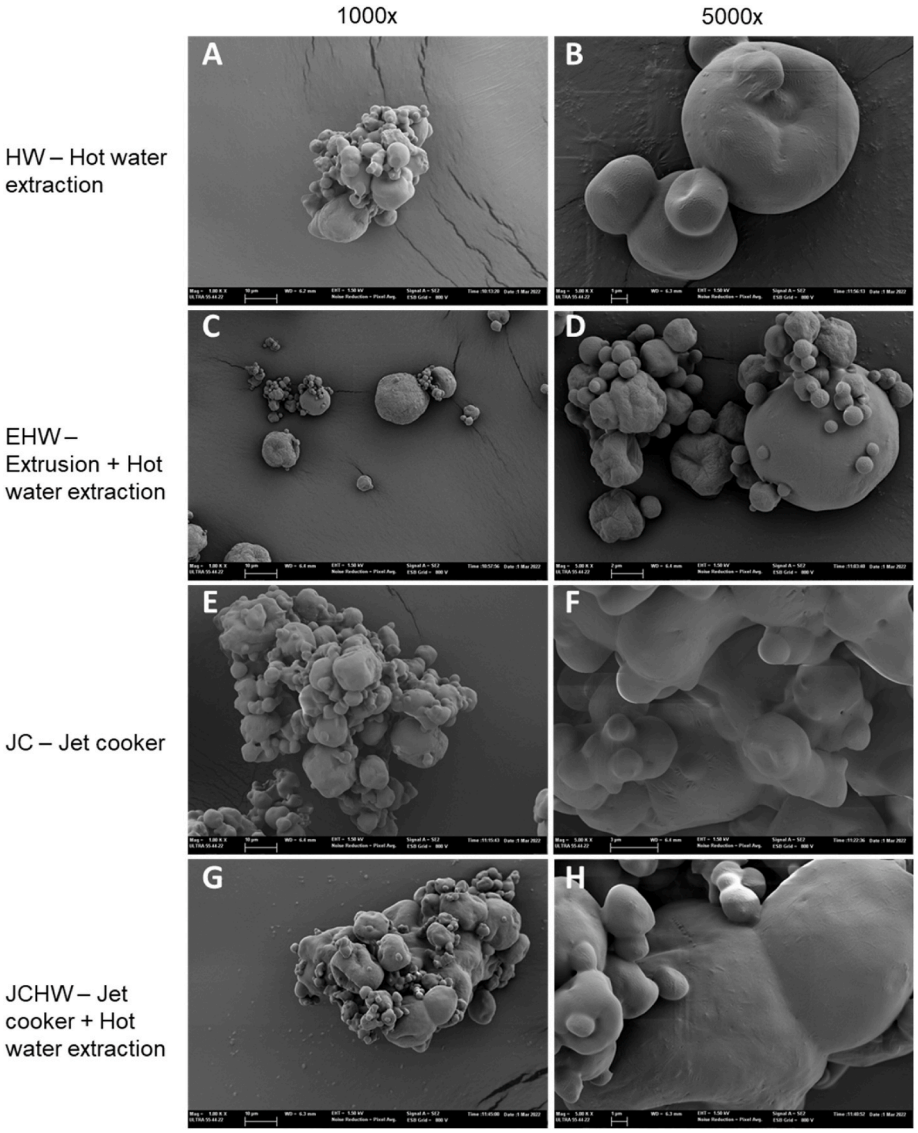

Fig. 2. Microstructure of the spray dried powders observed by FESEM.

content (46 g/100 g dwb in EHW compared to 60–65 g/100 g dwb in the other samples, according to Perez-Pirotto et al., 2022).

3.2. Color

Color values obtained for the four powders are exhibited on Table 1. The powder obtained under the extrusion treatment (EHW) was the one with the darkest color as indicated by the lowest L* value. Also, the browning index for this powder is the highest and significantly different ($p < 0.05$) from the others. Between the treatments assayed, the extrusion exposes the sample to the highest temperature, a condition that may favor non enzymatic browning reactions, such as caramelization or Maillard reactions. However, all browning indexes were lower than those observed by Phuon et al. (2021), for orange peels dried by different methods.

As a* and b* parameters are positive for all treatments, the four powders exhibit red and yellow shades, tending to have an orange tone. No significant differences ($p > 0.05$) were observed on a* values between HW and JC. On b* values, the only significantly different from the others was JCHW. Therefore, although on yellow shades they are all similar, JCHW powder has a lower red component, which is also shown on the highest L* and Hue angle values.

3.3. Particle size

Particle size distribution is shown in Fig. 3, and D_{10}, D_{50}, D_{90}, and span values are exhibited in Table 2.

As indicated by span values, HW and EHW gave more broader distributions, with a higher particle size range. JCHW gave the most homogeneous powder size, however it was the biggest one. Despite the difference on observed span values, all powders are mostly homogenous, as their span is around 1 in all cases.

As seen in section 3.1., JC and JCHW powders microstructure exhibit more caking than EHW and HW, which is clearly evidenced in sizes of the particles. Once they have established the liquid bridge, particles dissolute and form a bigger particle (Edrisi Sormoli & Langrish, 2016). In the case of EHW and HW, where aggregation is seen but not at such a degree, size is lower and also span values are higher, as each particle keeps its original size.

3.4. Moisture content, hydration properties and oil holding capacity

Moisture content is an important parameter to determine the powder stability during storage (Bhusari et al., 2014). It should be below 14% to prevent or minimize microbial growth and chemical deterioration (Mokhtar et al., 2018). All the powders had moisture contents below 6%, as shown on Table 3, being significantly lower ($p < 0.05$) for EHW and JC, with no significant difference between them ($p > 0.05$).

Table 1
Color properties of the different powders. HW: Hot water; EHW: Extrusion + hot water; JC: jet cooker; JCHW: jet cooker + hot water.

Treatment	L*	a*	b*	Hue angle	Chroma	Browning index
HW	81.07 ± 0.09^{b}	2.84 ± 0.02^{b}	24.13 ± 0.10^{b}	83.28 ± 0.07^{b}	24.30 ± 0.10^{b}	28.76 ± 0.21^{b}
EHW	78.46 ± 0.22^{a}	4.85 ± 0.17^{c}	24.41 ± 0.15^{b}	78.76 ± 0.37^{a}	24.89 ± 0.15^{b}	41.10 ± 0.32^{c}
JC	81.71 ± 1.11^{b}	2.58 ± 0.63^{b}	24.49 ± 1.15^{b}	84.03 ± 1.18^{b}	24.63 ± 1.20^{b}	37.24 ± 3.13^{b}
JCHW	84.84 ± 0.34^{c}	1.11 ± 0.17^{a}	21.00 ± 0.31^{a}	86.97 ± 0.43^{c}	21.03 ± 0.32^{a}	28.76 ± 0.73^{a}

Different letters in the same column indicate significant difference ($p < 0.05$). Results are expressed as mean ± SD of two repetitions.

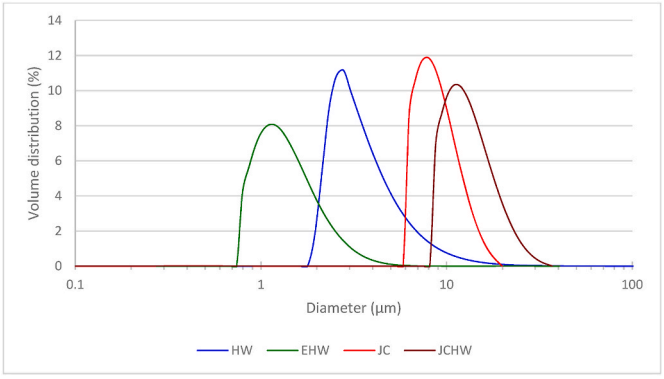

Fig. 3. Particle size of the different powders. HW: Hot water; EHW: Extrusion + hot water; JC: jet cooker; JCHW: jet cooker + hot water.

Table 2
Particle sizes of the different powders. HW: Hot water; EHW: Extrusion + hot water; JC: jet cooker; JCHW: jet cooker + hot water.

Treatment	D10 (μm)	D50 (μm)	D90 (μm)	Span
HW	1.86 ± 0.47^{a}	2.63 ± 0.68^{b}	5.21 ± 1.29^{b}	1.28 ± 0.02^{d}
EHW	0.76 ± 0.15^{a}	1.10 ± 0.22^{a}	1.97 ± 0.33^{a}	1.11 ± 0.05^{c}
JC	6.32 ± 0.02^{b}	8.34 ± 0.06^{c}	12.15 ± 0.01^{c}	0.70 ± 0.00^{b}
JCHW	16.95 ± 0.98^{c}	21.17 ± 0.76^{d}	28.07 ± 0.39^{d}	0.53 ± 0.04^{a}

Different letters in the same column indicate significant difference ($p < 0.05$). Results are expressed as mean ± SD of two repetitions.

Table 3
Moisture content, Water solubility, hygroscopicity and oil holding capacity (OHC) of different powders. HW: Hot water; EHW: Extrusion + hot water; JC: jet cooker; JCHW: jet cooker + hot water.

Treatment	Moisture content (%)	Water solubility (%)	Hygroscopicity (g moisture/100 g sample)	OHC (g oil/g sample)
HW	4.99 ± 0.22^{b}	85.43 ± 0.21^{b}	15.21 ± 0.29$^{a, b}$	3.12 ± 0.04^{a}
EHW	4.12 ± 0.03^{a}	90.44 ± 0.18^{c}	15.65 ± 0.35^{b}	3.41 ± 0.02^{b}
JC	4.42 ± 0.03^{a}	86.32 ± 1.42^{b}	15.28 ± 0.03$^{a, b}$	3.28 ± 0.13$^{a, b}$
JCHW	5.43 ± 0.35^{b}	83.04 ± 0.06^{a}	14.63 ± 0.18^{a}	3.36 ± 0.05^{b}

Different letters in the same column show significant difference ($p < 0.05$). Results are expressed as mean ± SD of two repetitions.

Hydration properties and oil holding capacity of the different powders are also presented on Table 3. In the three analyses (water solubility, hygroscopicity and OHC), the powder with the highest performance is EHW. As this powder has the smallest particle size (section 3.2)., its relationship surface/volume is higher, and the interface that is exposed to the surrounding environment (water, oil or moisture), is higher.

All powders show good solubility in water, being significantly highest ($p < 0.05$) in EHW and lowest in the case of JCHW (Table 3). Water solubility is positively correlated with soluble fibre content, therefore it is expectable that the powder with the highest fibre content is the most soluble (Gu et al., 2020), in this case EHW with 20.2 g/100 g total dietary fibre and JCHW with 13.0 g/100 g total dietary fibre (Perez-Pirotto et al., 2022).

Hygroscopicity is the ability of the powder to absorb moisture from the surroundings and cause stickiness (Wong et al., 2018). Higher values were observed in powders with the lowest moisture content. This is due to the gradient between moisture content of the surrounding environment with the powder.

OHC is important from a technological point of view, as it prevents fat loss during cooking and helps remove excess fat from foods (Gan et al., 2020). Also, it plays an important role in nutrition, where it can bind bile acids and increase their excretion, therefore helping reduce plasma cholesterol (Tosh & Yada, 2010). Oil holding capacity of samples can be seen in Table 3. Differences between samples may be related to fibre content, as higher fibre content renders a higher oil holding capacity (Wang et al., 2017).

3.5. Foaming capacity and stability

Foaming capacity and stability values can be seen in Fig. 4. Although at the beginning JC foaming capacity is similar to EHW, the latter is the most stable foam. All the other foams have disappeared after 30 min. As all powders have the same protein content (8 g/100 g, according to the WPI percentage used as encapsulating agent), differences in foaming capacity and stability could be due to polysaccharides content. By increasing viscosity, polysaccharides structure and stabilize lamellar water, retarding liquid drainage and air-bubbles coalescence. Also, they form a flexible film around the air bubbles, improving the foam formation (Dick et al., 2019). Therefore, EHW is expected to be the one with the most stable foam, as it is the one with the highest fibre content, and therefore, polysaccharides content, according to Perez-Pirotto et al., 2022.

3.6. Rheology

The four treatments exhibited a Bingham-like behaviour, Newtonian with yield stress. All models fit with r^2 values higher than 0.99. They all adjust to the equation $\sigma = \sigma_y + \eta_p\dot{\gamma}$, where σ_y represents yield stress and η_p is plastic viscosity. Viscosity values were significantly different ($p < 0.05$) for the four of them. Results are shown on Table 4.

Highest viscosity and yield stress values were observed for EHW, which may be due to the higher amount of soluble fibre present in the sample (Perez-Pirotto et al., 2022). Dietary fiber, especially the soluble type, is well known for providing viscosity and changing rheological properties of the mixtures to which it is added. This thickening property of these compounds is related to the ability polysaccharides have to entangle physically with solution constituents. A positive and non-linear relationship exists between molecular weight of the fibres in the solution and the viscosity (Dikeman & Fahey, 2006). Therefore, extrusion seems to be the treatment that gives the fibres with the highest molecular weight and jet cooking the lowest ones. This could be due to the jet cooking breaking these to a higher extent than desired, ultimately liberating free sugars and decreasing the amount of soluble fibre

Table 4
Yield stress and viscosity of the samples. HW: Hot water; EHW: Extrusion + hot water; JC: jet cooker; JCHW: jet cooker + hot water.

Treatment	σ_y (mPa)	η_p (cP)
HW	39.27 ± 0.27^a	6.02 ± 0.19^b
EHW	56.33 ± 1.82^b	25.46 ± 0.53^d
JC	37.76 ± 0.66^a	4.16 ± 0.03^a
JCHW	37.02 ± 0.25^a	7.13 ± 0.15^c

Different letters in the same column show significant difference ($p < 0.05$). Results are expressed as mean ± SD of two repetitions.

(Perez-Pirotto et al., 2022).

3.7. Differential scanning calorimetry

Thermograms obtained by DSC analysis are shown on Fig. 5. In all cases there is a clear shift in the heat flow curve, related to a change in the specific heat of the sample associated to the glass transition.

Glass transition temperature is the temperature at which an amorphous system changes from a glassy state to a rubbery one. It is related to stability, as changes from glassy to rubbery state decrease viscosity and therefore increase molecular mobility (Daza et al., 2016). Glass transition values ranged from 3.49 ± 0.35 to 15.32 ± 0.40 °C, for HW and EHW, respectively. No significant difference was found between JC and JCHW glass transition temperature, which had a mean of 6.77 ± 0.85 °C ($p > 0.05$). These values indicate that at room temperature all powders are in the rubbery state. Storing a product above its glass transition temperature may cause caking and agglomeration (Kaderides & Goula, 2017), which is clearly seen in the case of HW, JC and JCHW in Fig. 2.

Glass transition temperatures of protein - sugars mixture have been extensively studied, and it has been found that measured *Tg* mainly reflects that of the sugars in the system, as described by Fang & Bhandari, 2012. Also, the differences in this parameter may be due to water content of the powders and molecular weight of its constituents (Ahmed et al., 2010; Moghbeli et al., 2020). EHW has the highest glass transition temperature, as it is the powder with the least amount of sugars, lower moisture content and higher fibre content (Perez-Pirotto et al., 2022).

4. Conclusion

All products exhibit an orange shade and spheric microstructure, although caking is notorious in the case of HW, JC and JCHW. They all increase viscosity of water solution, while they do not change the behaviour of the solution (all Bingham fluids). Regarding foaming, they

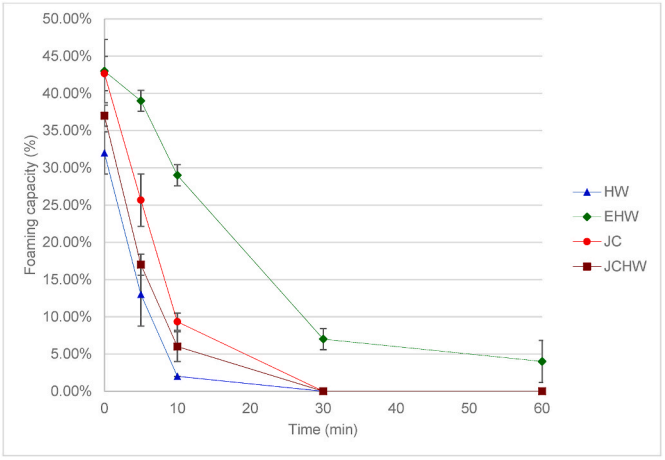

Fig. 4. Foam stability of solutions. HW: Hot water; EHW: Extrusion + hot water; JC: jet cooker; JCHW: jet cooker + hot water.

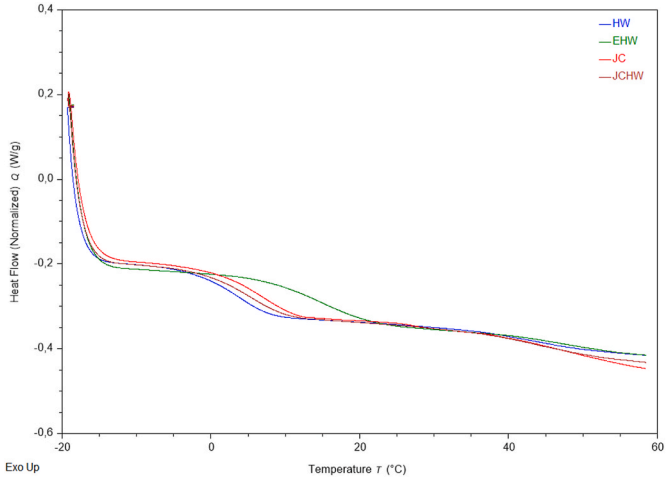

Fig. 5. DSC analytical curve of different powders. HW: Hot water; EHW: Extrusion + hot water; JC: jet cooker; JCHW: jet cooker + hot water.

all exhibit foaming capacity, but only EHW provides stability over time. This powder is also the most interesting from hydration properties and glass transition temperatures, as it is the one with the highest OHC, water solubility and glass transition temperature. Through valorization of a by-product and applying different extraction technologies, it was possible to obtain soluble fibre enriched powders that can be used as ingredients in the food industry due to their technofunctional characteristics.

Funding

This work was supported by the National Research and Innovation Agency (ANII), Uruguay, under code POS_EXT_2018_1_154449.

CRediT authorship contribution statement

Claudia Perez-Pirotto: Formal analysis, Investigation, Data curation, Writing – original draft, Project administration, Funding acquisition. **Gemma Moraga:** Methodology, Investigation, Writing – review & editing. **Amparo Quiles:** Methodology, Investigation, Writing – review & editing. **Isabel Hernando:** Conceptualization, Writing – review & editing, Supervision. **Sonia Cozzano:** Conceptualization, Methodology, Writing – review & editing, Supervision. **Patricia Arcia:** Conceptualization, Methodology, Writing – review & editing, Visualization, Supervision.

Declaration of competing interest

The authors declare no conflict of interest.

Acknowledgments

Authors are grateful to Novacore (Paysandú, Uruguay) for providing the orange pomace.

References

Ahmed, M., Akter, M. S., Lee, J. C., & Eun, J. B. (2010). Encapsulation by spray drying of bioactive components, physicochemical and morphological properties from purple sweet potato. *LWT - Food Science and Technology, 43*(9), 1307–1312. https://doi.org/10.1016/j.lwt.2010.05.014

Bhusari, S. N., Muzaffar, K., & Kumar, P. (2014). Effect of carrier agents on physical and microstructural properties of spray dried tamarind pulp powder. *Powder Technology, 266*, 354–364. https://doi.org/10.1016/j.powtec.2014.06.038

Chemat, F., Vian, M. A., & Cravotto, G. (2012). Green extraction of natural products: Concept and principles. *International Journal of Molecular Sciences, 13*(7), 8615–8627. https://doi.org/10.3390/ijms13078615

Daza, L. D., Fujita, A., Fávaro-Trindade, C. S., Rodrigues-Ract, J. N., Granato, D., & Genovese, M. I. (2016). Effect of spray drying conditions on the physical properties of Cagaita (Eugenia dysenterica DC.) fruit extracts. *Food and Bioproducts Processing, 97*, 20–29. https://doi.org/10.1016/j.fbp.2015.10.001

Dhingra, D., Michael, M., Rajput, H., & Patil, R. T. (2012). Dietary fibre in foods: A review. *Journal of Food Science & Technology, 49*(3), 255–266. https://doi.org/10.1007/s13197-011-0365-5

Dick, M., Dal Magro, L., Rodrigues, R. C., de Rios, A. O., & Flôres, S. H. (2019). Valorization of Opuntia monacantha (Willd.) Haw. cladodes to obtain a mucilage with hydrocolloid features: Physicochemical and functional performance. *International Journal of Biological Macromolecules, 123*, 900–909. https://doi.org/10.1016/j.ijbiomac.2018.11.126

Dikeman, C. L., & Fahey, G. C. (2006). Viscosity as related to dietary fiber: A review. *Critical Reviews in Food Science and Nutrition, 46*(8), 649–663. https://doi.org/10.1080/10408390500511862

Edrisi Sormoli, M., & Langrish, T. A. G. (2016). Spray drying bioactive orange-peel extracts produced by Soxhlet extraction: Use of WPI, antioxidant activity and moisture sorption isotherms. *LWT - Food Science and Technology, 72*, 1–8. https://doi.org/10.1016/j.lwt.2016.04.033

Elleuch, M., Bedigian, D., Roiseux, O., Besbes, S., Blecker, C., & Attia, H. (2011). Dietary fibre and fibre-rich by-products of food processing: Characterisation, technological functionality and commercial applications: A review. *Food Chemistry, 124*(2), 411–421. https://doi.org/10.1016/j.foodchem.2010.06.077

Fang, Z., & Bhandari, B. (2012). Comparing the efficiency of protein and maltodextrin on spray drying of bayberry juice. *Food Research International, 48*(2), 478–483. https://doi.org/10.1016/j.foodres.2012.05.025

Ferrari, C. C., Germer, S. P. M., & de Aguirre, J. M. (2012). Effects of spray-drying conditions on the physicochemical properties of blackberry powder. *Drying Technology, 30*(2), 154–163. https://doi.org/10.1080/07373937.2011.628429

Figueroa, L. E., & Genovese, D. B. (2019). Fruit jellies enriched with dietary fibre: Development and characterization of a novel functional food product. *LWT - Food Science and Technology, 111*, 423–428. https://doi.org/10.1016/j.lwt.2019.05.031

Fournaise, T., Petit, J., & Gaiani, C. (2021). Main powder physicochemical characteristics influencing their reconstitution behavior. *Powder Technology, 383*, 65–73. https://doi.org/10.1016/j.powtec.2021.01.056

Gagneten, M., Corfield, R., Mattson, M. G., Sozzi, A., Leiva, G., Salvatori, D., & Schebor, C. (2019). Spray-dried powders from berries extracts obtained upon several processing steps to improve the bioactive components content. *Powder Technology, 342*, 1008–1015. https://doi.org/10.1016/j.powtec.2018.09.048

Gan, J., Huang, Z., Yu, Q., Peng, G., Chen, Y., Xie, J., Nie, S., & Xie, M. (2020). Microwave assisted extraction with three modifications on structural and functional properties of soluble dietary fibers from grapefruit peel. *Food Hydrocolloids, 101*. https://doi.org/10.1016/j.foodhyd.2019.105549

Gao, J., Lin, L., Sun, B., & Zhao, M. (2017). A comparison study on polysaccharides extracted from: Laminaria japonica using different methods: Structural characterization and bile acid-binding capacity. *Food & Function, 8*(9), 3043–3052. https://doi.org/10.1039/c7fo00218a

Gu, M., Fang, H., Gao, Y., Su, T., Niu, Y., Yu, L., & Lucy). (2020). Characterization of enzymatic modified soluble dietary fiber from tomato peels with high release of lycopene. *Food Hydrocolloids, 99*, Article 105321. https://doi.org/10.1016/j.foodhyd.2019.105321

Guo, Y., Liu, W., Wu, B., Wu, P., Duan, Y., Yang, Q., & Ma, H. (2018). Modification of garlic skin dietary fiber with twin-screw extrusion process and in vivo evaluation of Pb binding. *Food Chemistry, 268*, 550–557. https://doi.org/10.1016/j.foodchem.2018.06.047

Gutiérrez Barrutia, M. B., Curutchet, A., Arcia, P., & Cozzano, S. (2019). New functional ingredient from orange juice byproduct through a green extraction method. *Journal of Food Processing and Preservation, 43*(5), 1–8. https://doi.org/10.1111/jfpp.13934

Huang, Y. L., & Ma, Y. S. (2016). The effect of extrusion processing on the physiochemical properties of extruded orange pomace. *Food Chemistry, 192*, 363–369. https://doi.org/10.1016/j.foodchem.2015.07.039

Kaderides, K., & Goula, A. M. (2017). Development and characterization of a new encapsulating agent from orange juice by-products. *Food Research International, 100*, 612–622. https://doi.org/10.1016/j.foodres.2017.07.057

Liang, X., Ran, J., Sun, J., Wang, T., Jiao, Z., He, H., & Zhu, M. (2018). Steam-explosion-modified optimization of soluble dietary fiber extraction from apple pomace using response surface methodology. *CyTA - Journal of Food, 16*(1), 20–26. https://doi.org/10.1080/19476337.2017.1333158

Li, B., Yang, W., Nie, Y., Kang, F., Goff, H. D., & Cui, S. W. (2019). Effect of steam explosion on dietary fiber, polysaccharide, protein and physicochemical properties of okara. *Food Hydrocolloids, 94*, 48–56. https://doi.org/10.1016/j.foodhyd.2019.02.042

Majerska, J., Michalska, A., & Figiel, A. (2019). A review of new directions in managing fruit and vegetable processing by-products. *Trends in Food Science & Technology, 88*, 207–219. https://doi.org/10.1016/j.tifs.2019.03.021

Moczkowska, M., Karp, S., Niu, Y., & Kurek, M. A. (2019). Enzymatic, enzymatic-ultrasonic and alkaline extraction of soluble dietary fibre from flaxseed – a physicochemical approach. *Food Hydrocolloids, 90*, 105–112. https://doi.org/10.1016/j.foodhyd.2018.12.018

Moghbeli, S., Jafari, S. M., Maghsoudlou, Y., & Dehnad, D. (2020). A Taguchi approach optimization of date powder production by spray drying with the aid of whey protein-pectin complexes. *Powder Technology, 359*, 85–93. https://doi.org/10.1016/j.powtec.2019.10.013

Mokhtar, S. M., Swailam, H. M., & Embaby, H. E. S. (2018). Physicochemical properties, nutritional value and techno-functional properties of goldenberry (Physalis peruviana) waste powder concise title: Composition of goldenberry juice waste. *Food Chemistry, 248*, 1–7. https://doi.org/10.1016/j.foodchem.2017.11.117

O'Keefe, S. J. (2019). The association between dietary fibre deficiency and high-income lifestyle-associated diseases: Burkitt's hypothesis revisited. *The Lancet Gastroenterology and Hepatology, 4*(12), 984–996. https://doi.org/10.1016/S2468-1253(19)30257-2

Oliveira, B. E., Junior, P. C. G., Cilli, L. P., Contini, L. R. F., Venturini, A. C., Yoshida, C. M. P., & Braga, M. B. (2018). Spray-drying of grape skin-whey protein concentrate mixture. *Journal of Food Science & Technology, 55*(9), 3693–3702. https://doi.org/10.1007/s13197-018-3299-3

Perez-Pirotto, C., Cozzano, S., Hernando, I., & Arcia, P. (2022). Different green extraction technologies for soluble dietary fibre extraction from orange by-product. *International Journal of Food Science and Technology*. https://doi.org/10.1111/ijfs.15756

Phuon, V., Ramos, I. N., Brandão, T. R. S., & Silva, C. L. M. (2021). Assessment of the impact of drying processes on orange peel quality characteristics. *Journal of Food Process Engineering*. https://doi.org/10.1111/jfpe.13794

Quiles, A., Campbell, G. M., Struck, S., Rohm, H., & Hernando, I. (2018). Fiber from fruit pomace: A review of applications in cereal-based products. *Food Reviews International, 34*(2), 162–181. https://doi.org/10.1080/87559129.2016.1261299

Rodríguez, R., Jiménez, A., Fernández-Bolaños, J., Guillén, R., & Heredia, A. (2006). Dietary fibre from vegetable products as source of functional ingredients. *Trends in Food Science & Technology, 17*(1), 3–15. https://doi.org/10.1016/j.tifs.2005.10.002

Santos, D., Lopes da Silva, J. A., & Pintado, M. (2022). Fruit and vegetable by-products' flours as ingredients: A review on production process, health benefits and technological functionalities. *LWT - Food Science and Technology, 154*. https://doi.org/10.1016/j.lwt.2021.112707

Soukoulis, C., Lebesi, D., & Tzia, C. (2009). Enrichment of ice cream with dietary fibre: Effects on rheological properties, ice crystallisation and glass transition phenomena. *Food Chemistry, 115*(2), 665–671. https://doi.org/10.1016/j.foodchem.2008.12.070

Tosh, S. M., & Yada, S. (2010). Dietary fibres in pulse seeds and fractions: Characterization, functional attributes, and applications. *Food Research International, 43*(2), 450–460. https://doi.org/10.1016/j.foodres.2009.09.005

Wang, T., Liang, X., Ran, J., Sun, J., Jiao, Z., & Mo, H. (2017). Response surface methodology for optimisation of soluble dietary fibre extraction from sweet potato residue modified by steam explosion. *International Journal of Food Science and Technology, 52*(3), 741–747. https://doi.org/10.1111/ijfs.13329

Wang, L., Xu, H., Yuan, F., Fan, R., & Gao, Y. (2015). Preparation and physicochemical properties of soluble dietary fiber from orange peel assisted by steam explosion and dilute acid soaking. *Food Chemistry, 185*, 90–98. https://doi.org/10.1016/j.foodchem.2015.03.112

Wilkins, M. R., Suryawati, L., Maness, N. O., & Chrz, D. (2007). Ethanol production by Saccharomyces cerevisiae and Kluyveromyces marxianus in the presence of orange-peel oil. *World Journal of Microbiology and Biotechnology, 23*(8), 1161–1168. https://doi.org/10.1007/s11274-007-9346-2

Wong, C. W., Teoh, C. Y., & Putri, C. E. (2018). Effect of enzymatic processing, inlet temperature, and maltodextrin concentration on the rheological and physicochemical properties of spray-dried banana (Musa acuminata) powder. *Journal of Food Processing and Preservation, 42*(2), 1–9. https://doi.org/10.1111/jfpp.13451

Xie, F., Li, M., Lan, X., Zhang, W., Gong, S., Wu, J., & Wang, Z. (2017). Modification of dietary fibers from purple-fleshed potatoes (heimeiren) with high hydrostatic pressure and high pressure homogenization processing: A comparative study. *Innovative Food Science & Emerging Technologies, 42*, 157–164. https://doi.org/10.1016/j.ifset.2017.05.012

Zhang, W., Zeng, G., Pan, Y., Chen, W., Huang, W., Chen, H., & Li, Y. (2017). Properties of soluble dietary fiber-polysaccharide from papaya peel obtained through alkaline or ultrasound-assisted alkaline extraction. *Carbohydrate Polymers, 172*, 102–112. https://doi.org/10.1016/j.carbpol.2017.05.030

Zhong, L., Fang, Z., Wahlqvist, M. L., Hodgson, J. M., & Johnson, S. K. (2019). Extrusion cooking increases soluble dietary fibre of lupin seed coat. *LWT - Food Science and Technology, 99*, 547–554. https://doi.org/10.1016/j.lwt.2018.10.018